DRUG ANALYTICAL RESEARCH
ISSN: 2527-2616 *www.seer.ufrgs.br/dar*

Hydrogels containing spray-dried avobenzone and resveratrol-loaded nanocapsules using titanium dioxide and microalgae as drying adjuvants: an innovative formulation for photoprotection

Gabryelle Furtado de Almeida[a]*, Manuela de Castilhos França Gonçalves[a], Lana Flavia Baron[a], Mariana Büttenbender[a], Kelly Cristine Zatta[a], Max Seidy Saito[a], Silvia Maria Mathes Faustino[e], Karina Paese[a], Adriana Raffin Pohlmann[a,b] and Silvia Stanisçuaski Guterres[a,c,d]

[a]Programa de Pós-Graduação em Ciências Farmacêuticas, Universidade Federal do Rio Grande do Sul, Porto Alegre, Brazi;[b]Departamento de Química Orgânica, Instituto de Química, Universidade Federal do Rio Grande do Sul, Porto Alegre, RS, Brazil; [c]Programa de Pós-Graduação em Nanotecnologia Farmacêutica, Universidade Federal do Rio Grande do Sul, Porto Alegre, Brazil; [d]Programa de Pós-Graduação em Farmácia, Faculdade de Farmácia, Universidade Federal da Bahia, Salvador, BA, Brazil; [e]Laboratório de Cultivo de Microalgas, Faculdade de Farmácia, Universidade Federal do Amapá, Macapá, AP, Brazil.
** Corresponding author: gabryelle.almeida@gmail.com*

Photoprotective substances are needed to minimize the harmful effects of UV radiation on the skin. In this context, the objective of this work was to develop and characterize a hydrogel containing spray-dried avobenzone and resveratrol loaded nanocapsules using titanium dioxide and microalgae as drying adjuvants. The nanocapsules, previously developed and characterized, were dried using the spray drying technique with the aid of titanium dioxide (3% w/v) and/or a mixture of it (2.7% w/v) with the microalgae of the species *Scenedesmus ecornis* as excipients (0.3% w/v). The powders showed good yields (67-70%), with low moisture content (<1.5%) and average particle size in the micrometer range (>30 µm). The drying process of spray-dried powders did not significantly affect the content of avobenzone and resveratrol (above 85% for both), although the morphological description indicates the presence of micro-agglomerates. Subsequently, the powders were incorporated into hydrophilic gels prepared with sodium acrylates copolymer and lecithin. Then, the hydrogel containing spray-dried avobenzone and resveratrol loaded nanocapsules was produced and characterized using titanium dioxide and microalgae (HG-$NC_{A+R+TiM}$) as a drying adjuvant. The formulation was evaluated for irritability by HET-CAM, permeation/penetration of avobenzone, washability profile and in vitro efficacy. The hydrogel presented a pH value of 7.52, drug content of 1.24% for avobenzone (w/w) and 0.04% for resveratrol (w/w), and a non-Newtonian pseudoplastic rheological behavior. The free avobenzone from a hydrogel and from HG-$NC_{A+R+TiM}$ did not permeate the skin layers. The evaluation by HET-CAM did not detect irritating reactions of the formulation. The structure of HG-$NC_{A+R+TiM}$ allowed a greater resistance to the washing flow indicating good adhesive capacity on the skin surface in comparison to the free hydrogel. The in vitro efficacy test showed that HG-$NC_{A+R+TiM}$ absorbed and spreaded the UV light with maximum wavelengths in the erythematous range (305-328 nm). In conclusion, these spray-dried powders are promising formulations to be incorporated into photoprotective hydrogels intended for cutaneous administration.

Keywords: Avobenzone; Hydrogel; Microalgae; Microparticles; Photoprotectors, HPLC.

Article received at 05/17/2025 and accepted at 07/15/2025.
https://doi.org/10.22456/2527-2616.147538

Introduction

The skin is one of the main surfaces of interaction with the environment and it is subject to aging, a complex and multifactorial biological process. One of the causes of the acceleration of skin aging is the accumulated and unprotected sun exposure (1). The layers of skin are more sensitive to ultraviolet (UV) radiation, especially to the UVA and UVB bands. The UVB radiation (290-320 nm) has high energy and about 5% of reach Earth's surface. The UVA radiation (320-400 nm) has lower energy, about 95% reach Earth's surface and can penetrate deep into the layers of the skin, reaching the dermis and inducing pigmentation, causing undesirable effects such as allergies, skin aging and skin cancer. It appears that both UVB and UVA radiation trigger similar mechanisms that lead to inflammation and then immunosuppression in the skin. (2). In addition, excessive UV exposure can cause the formation of reactive oxygen species (oxidative stress), which are a primary factor in inducing skin damage (protein, lipid, and cellular DNA) contributing to photoaging (3,4).

In recent years, the care with appearance and skin health reflects on the increase of the cosmetic products consume. Among the products, sunscreen formulations stand out, which are widely studied due to its limited chemical stability and the need to modulate the cutaneous permeation/penetration of most of the commercially available sunscreens (5). The avobenzone (4-tert-butyl-4′-methoxydibenzoylmethane), a photosensitive substance with UVA filter action, is one of the most used in photoprotective formulations, although there is much discussion about the problems of photostability and

incompatibility with other filters. Currently, avobenzone is the only substance approved worldwide by the FDA for use in sunscreens (6).

In recent years, the development of formulations with an emphasis on nanotechnological innovations has significantly transformed several aspects of the cosmetic industry (7). Additionally, the use of natural compounds with antioxidant effects in photoprotective formulations, combined with nanoparticles, is a promising approach. Resveratrol is a stilbene molecule belonging to the polyphenol family, widely used in therapeutic strategies due to its antioxidant properties. On the other hand, resveratrol is sensitive to light, pH and temperature rise due to its unstable hydroxyls and a double C=C bond (8). Recently, studies have shown an improvement of resveratrol photostability after encapsulation in different nanostructures (9), an increase in its antioxidant activity and photostability after co-encapsulation of resveratrol and curcumin (10) and potentiation of the antioxidant activity in the co-nanoencapsulation of resveratrol and lipoic acid (11).

The use of mechanisms and systems that improve the quality of the end product is fundamental in view of the problems and disadvantages listed on the performance of sunscreens. Thus, a feasible alternative is the drying of the nanocapsule suspensions to increase the physical stability, prolong the shelf life and minimize the microbiological contamination (12,13). Furthermore, the use of an appropriate drying adjuvant is crucial to ensure the efficiency of the spray drying process, which directly influences the quality of the powder (14). It is worth mentioning that our research group was the precursor in the development of drying techniques of polymeric nanocapsules using spray-drying techniques and different drying adjuvants. (15).

Despite that, the use of titanium dioxide as a drying adjuvant is not yet properly studied, as well as its association with microalgae of the genus *Scenedesmus spp*. Microalgae show high biomass production (16,17), with emphasis on lipid productivity and a higher frequency of fatty acids (18). Additionally, they also present as a defense mechanism the synthesis of photoprotective compounds (mycosporine-like amino acids) that absorb UV radiation, being interesting for formulations in cosmetic use (19). Considering this, the aim of this study was to develop and characterize a hydrogel composed of spray-dried nanocapsules containing avobenzone and resveratrol previously dried using titanium dioxide associated with microalgae. Therefore, our hypothesis was that the set of components of the hydrogel could increase adhesion and modulate the penetration / permeation of avobenzone in the skin.

Experimental section

Materials

Avobenzone was obtained from Jovii Cosmecêutica (Cachoeirinha, Brazil). Resveratrol was acquired from Dermogral (Porto Alegre, Brazil). Poly(ε-caprolactone) (PCL) (MW 80,000) and sorbitan monostearate were purchased from Sigma-Aldrich (São Paulo, Brazil). Polysorbate 80, ethanol and acetone were obtained from Vetec (Rio de Janeiro, Brazil). The capric/caprylic triglyceride was purchased from Delaware (Porto Alegre, Brazil). Titanium dioxide (Eusolex® T-AVO) was obtained from Merck (São Paulo, Brazil). All other chemicals and solvents used were of analytical or pharmaceutical grade and used as received.

Collection, isolation, and identification of microalgae

The microalgae samples were collected from lakes and/or rivers in the city of Macapá-AP (Brazil) with the aid of a phytoplankton net of 20 µm. Horizontal drag was performed on the surface of the water column. Then, they were isolated by diluting the sample (1:1) with distilled water in slides and observed by optical microscopy (400x) to identify the species based on reports in the literature (20). Subsequently, they were grown in the laboratory.

Culture medium and microalgae growth conditions

The culture medium used was NPK (Nitrogen, Phosphorus and Potassium) in the following proportions: N solution in water 15%; P_2O_5 solution in water 5% and K_2O solution in water 5%. The choice of this medium was influenced by the cost/effectiveness ratio. The microalgae cultures were subjected to constant aeration, light intensity equivalent to 32 µmol $m^{-2}s^{-1}$, photoperiod of 12h and temperature of 25 ºC. Cultivation time was determined based on species productivity.

Drying of microalgae biomass

The drying of the biomass was done through lyophilization of the wet biomass. Firstly, the samples were decanted for 24 hours in microbiological flasks and then, the residual biomass was transferred to petri dishes and identified for freezing later. The microalgae were lyophilized for 12h. At the end of the process, they presented a granular aspect of green color.

Methods

Development of nanocapsule suspensions containing avobenzone and resveratrol

Preparation of nanocapsules

The nanocapsules were prepared in the form of colloidal suspension, using the method of interfacial deposition of preformed polymer adapted from Venturini et al, (2011) (21). Avobenzone (0.025 g), resveratrol (0.005 g), sorbitan monostearate (0.038 g), PCL (0,100 g) and capric/caprylic triglycerides (0.16 mL) were dissolved in acetone (23 mL) and ethanol (4 mL) at 48ºC. Subsequently, the organic phase was injected into the

aqueous phase (53 mL) with polysorbate 80 (0.038 g) under magnetic stirring. After 10 minutes, acetone was eliminated, and the suspension concentrated to a final volume of 10 mL under reduced pressure at 40ºC. A suspension of nanocapsules was also prepared without avobenzone and resveratrol and called LNC-B (lipid-core nanocapsules suspensions without active). The formulations were prepared in triplicate batches and stored at room temperature.

Characterization of lipid-core nanocapsules

All nanocapsules formulations were evaluated considering the average diameter in relation to the equivalent sphere volume (d4,3), using laser diffraction (Malvern® 2000 Mastersizer, Malvern Instruments, United Kingdom) with refractive index of PCL (1,46). Particle size (hydrodynamic diameter z-average), polydispersity index (PDI) and zeta potential were analyzed using dynamic light scattering (ZetaSizer® nano ZS, Malvern Instruments, United Kingdom). For diameter analysis, the samples were diluted 500 times (v/v) in ultrapure water. For the measurement of zeta potential, the formulations were diluted 500x in 10 mM aqueous NaCl (sodium chloride) solution and analyzed. The determination of pH was carried out in a potentiometer (D-22, Digimed, Brazil) previously calibrated with buffer solution pH 4.0 and 7.0, immersed directly in the colloidal suspensions.
The quantification of avobenzone was performed using high-performance liquid chromatography (HPLC), according to adapted methodology (22). The chromatographic system consisted of a C_{18} column (250 mm x 4.6 mm, 5 µm particle size, Phenomenex) and HPLC equipment (Shimadzu, Kyoto, Japan). The mobile phase used was a composition of acetonitrile solvent and water 90:10 (v/v) acidified with 1% acetic acid (w/v), with isocratic elution of 1.0 mL/min, detection wavelength of 360 nm and the injection volume of 30 µL.
The quantification of resveratrol was performed by HPLC equipment (Shimadzu, Kyoto, Japan) using a C_{18} column (150 mm x 4.6 mm, 5 µm particle size, Phenomenex), with mobile phase composed of acetonitrile and water 35:65 (v/v) and apparent pH adjusted to 3.0 with 10% orthophosphoric acid. The isocratic flow used was 1.2 mL/min with detection at a wavelength of 306 nm and an injection volume of 20 µL, according to adapted methodology (23). The ultrafiltration-centrifugation technique was used determine the concentration of avobenzone and resveratrol in the outer phase of the formulations (lipid-core nanocapsules containing avobenzone - LNC-AVO, lipid-core nanocapsules containing avobenzone and resveratrol - LNC-AVO+RSV. All measures were carried in triplicate. For this, aliquots of 400 µL of the nanosuspensions containing avobenzone and resveratrol were inserted into Millipore® 10,000Da membrane and centrifuged in 1840x g for 5 minutes (24). Posteriorly, 50 µL of each ultrafiltrate was injected in the HPLC for quantification of avobenzone and resveratrol.

Preparation of spray-dried nanocapsules using titanium dioxide and microalgae as drying adjuvant

The lipid-core nanocapsule suspensions were spray-dried using titanium dioxide, and with a mixture of titanium dioxide and microalgae as a drying adjuvant. The drying procedure was divided into groups as follows: The first group was LNC-B, LNC-AVO and LNC-AVO+RSV dried with titanium dioxide 3% (w/v); and the second group was LNC-AVO and LNC-AVO+RSV were dried with titanium dioxide 2.7% (w/v) and microalgae 0.3% (w/v); each formulation were prepared in triplicate batch. All suspensions were kept under magnetic stirring for 30 min with their respective drying adjuvant and then taken to drying (Büchi B290, Switzerland). The process parameters were inlet temperature of 120 ºC; outlet temperature (70 ± 5 °C) compressed air flow of 60 L/h, 0,5 mL/min of sample feed rate and aspiration 0.6 m^3/min.

Characterization of spray-dried powders

The process yield (%) was calculated as the ratio between the total weight of powder recovered in the sample collector and all solid components of the formulation (triplicate). The residual moisture content (%) of each spray-dried product was measured by an infrared moisture analyzer (Ohaus MB45, Parsippany, USA).
Morphology of powders was visualized through scanning electron microscopy at 10 kV (SEM; JEOL, JSM 6060, Tokyo, Japan). Therefore, the samples were fixed in aluminum stubs and sputter-coated with gold. The analysis was performed at the Centro de Centro de Microscopia e Microanálise - UFRGS (Porto Alegre, Brazil).
The size of the spray-dried powder particles was measured using laser diffraction by wet dispersion (Hydro 2000SM-AWM2002, Malvern, United Kingdom), using isooctane as solvent in sufficient quantity to achieve an obscuration between 2 and 8%. The analyzes were made considering the refractive indices of the polymer (1.46) and titanium dioxide (2.61).
In order to quantify the avobenzone and resveratrol content of powders, the samples were dispersed in a solution of acetonitrile and water 90:10 (v/v) and a solution of acetonitrile and water 50:50 (v/v), respectively, kept under magnetic stirring for 2 min. Then, the samples were taken to ultrasound bath for 30 min, and then centrifuged for 10 min at 4000 rpm. The supernatants were filtered (0.45 µm - Millipore® Millex-GV), and avobenzone and resveratrol were quantified by HPLC according to the method described above.

Incorporation of the spray-dried powders in the hydrogel

Five different powders were developed and each one was incorporated into a different hydrogel containing 1%

(w/w) of spray dried powder (hydrogel containing spray-dried blank nanocapsules using only TiO_2 as the drying adjuvant (HG-NC_{B+Ti}); hydrogel containing spray-dried avobenzone nanocapsules using only TiO_2 as the drying adjuvant (HG-NC_{A+Ti}); hydrogel containing spray-dried avobenzone nanocapsules using TiO_2 and microalgae as the drying adjuvant (HG-NC_{A+TiM}); hydrogel containing spray-dried avobenzone and resveratrol nanocapsules using only TiO_2 as the drying adjuvant (HG-NC_{A+R+Ti}); and hydrogel containing spray-dried avobenzone and resveratrol nanocapsules using TiO_2 and microalgae as the drying adjuvant (HG-$NC_{A+R+TiM}$). For the preparation of the hydrogel, spray dried powder (1.00%) and imidazolidinyl urea (0.12%) were levigated with propylene glycol (3.00%) and incorporated into Lecigel™ (sodium acrylates copolymer and lecithin) (0.25 %) with water to the final volume of 25 g of hydrogel. At the end, the hydrogel was stored under refrigeration in a refrigerator at 6 ºC. In addition, two hydrogels were developed: one containing the gelling polymer with the preservative dispersed in water (HG-B), used as a "blank" formulation, without active substances; and the other was produced through dispersion of the polymer in water together with avobenzone (0.06%), resveratrol (0.01%), imidazolidinyl urea (0.12%) and ethanol (8.00%); this was used as a free hydrogel (HG-FREE).

Characterization of hydrogels

The contents of avobenzone and resveratrol in the hydrogels were quantified by HPLC according to the method described above. For this, a predetermined amount of each hydrogel was added in a 10 mL volumetric flask. The extraction procedure for each analyzed substance, avobenzone and resveratrol, was performed respectively in its mobile phase. Then, the samples were taken to ultrasound for 30 min and then filtered (0.45 µm) and analyzed by HPLC.
The pH of formulations was characterized using a calibrated potentiometer (DM-22, Digimed, Brazil) after the dispersion of an aliquot of hydrogels in ultrapure water (1:10 w/v). The particle sizes of the hydrogels were assessed by laser diffraction (Mastersizer 2000®, Malvern Instruments, United Kingdom). The refractive index of the polymer (1.46) and titanium dioxide (2.61) were used for the analysis of hydrogels. The morphology was visualized through scanning electron microscopy (SEM; JEOL, JSM-6060, Japan).

Determination of rheological behavior

The rheological characteristics of semi-solid formulations (HG-$NC_{A+R+TiM}$ and HG-B) were evaluated 24 hours after preparation, using a rotational viscometer (Brookfield DV-II + Pro spindle SC4-25). The samples were kept at 25 ± 2ºC during the analysis. The spindle's rotation speed was predetermined based on the torque values (between 10 and 100%). The data obtained were applied to the equations (described below) that represent different rheological models: Bingham, Casson, Ostwald and Herschel-Bulkley. The model with the highest correlation coefficient was selected to represent the behavior of the formulations.

$$\text{Bingham} \rightarrow \tau = \tau o + \eta \dot{\gamma} > \text{Bingham plastic}$$
$$\text{Casson} \rightarrow \tau^{0.5} = \tau o^{0.5} + \eta \dot{\gamma}^{0.5} > \text{plastic}$$
$$\text{Ostwald} \rightarrow \tau = K \dot{\gamma}^{n} > \text{pseudoplastic flux}$$
$$\text{Herschel-Bulkley} \rightarrow \tau = \tau o + K \dot{\gamma}^{n} > \text{pseudoplastic flux with yield stress}$$

Where, τ is stress share, τo is initial stress share, $\dot{\gamma}$ is stress rate, η is flow index, η is viscosity and K is consistency index (Pas^{-n}).

Evaluation of avobenzone skin penetration/permeation

The end formulations (HG-$NC_{A+R+TiM}$ and HG-FREE) were conducted to the penetration/permeation study (n=6) using Franz vertical diffusion cells (Hanson Research, Chatsworth, California, USA), using pig ear skin as a model membrane. The natural membrane was kept in contact with a receptor solution composed of phosphate buffer pH 7.4 plus polysorbate 80 to 2% (w/v) considering the sink condition, at a temperature of 32 ºC ± 0.5 ºC, being the lower compartment constantly stirred with a magnetic bar.
The hydrogel samples (200 mg) were applied over the natural membrane corresponding to 280 µg/cm^2 of avobenzone and left in contact with the porcine skin for a period of 24 hours under the infinite dose principle. At predetermined times (30 min, 2h, 6h, 12h, 16h, 20h and 24h) an aliquot of 1.0 mL was collected from the receptor medium and avobenzone was quantified using the analytical methodology described above. After this period, the diffusion cells were disassembled and each area exposed to the samples was washed with ultrapure water and analyzed for the content of the avobenzone retained in the stratum corneum, epidermis/dermis and in the receiving solution. The specificity test was performed and confirmed that there was no interference of any substance of the pig ear skin in the retention time of avobenzone in the chromatographic run.

Skin layer separation procedure

The tape stripping technique was used to analyze the avobenzone content in the stratum corneum. Therefore, consecutive layers of stratum corneum were removed, adhering strips of adhesive tape (Scotch 3M, Porto Alegre, Brazil) to the area previously exposed to the samples. Ten fractions of adhesive tape were used to extract the stratum corneum. The 10 tapes were placed in a test tube containing 10 mL of the extractor medium (mobile phase - acetonitrile and water 90: 10 (v/v) acidified with 1% (v/v) acetic acid) and were subjected to extraction using vortex (2 min) and sonication (30 min). After this process, the samples were filtered (0.45 µm)

and subjected to assay using analytical methodology previously validated (25).
After removal of the stratum corneum, an epidermis was separated from the dermis, submerging the skin in ultrapure water at 65 ºC for 45 seconds. After that, the epidermis was removed with a scalpel and subjected to an extraction process, like the stratum corneum, however with 3 mL of the solvent extractor. The remaining dermis was crushed and submitted to a process of extraction using vortex (2 min) and sonication (30 min). After this procedure, the samples were filtered (0.45 µm), and the filtrate was subjected to assay by the analytical method described above (25).

Determination of the irritation potential

To evaluate the irritation potential of formulations (HG-$NC_{A+R+TiM}$, HG-FREE and HG-B), hen´s egg chorioallantoic membrane test was performed with fertile chicken eggs (26), on the 10th day of incubation. Egg shells were opened at the air cell and the white membrane was removed. To apply the hydrogels under the membrane, the samples were diluted in ultrapure water in a ratio 1:1 (v/v) and stirred by vortex for one minute. 600 µL of the formulation was applied on the chorioallantoic membrane and after 20 seconds the membrane was rinsed with saline solution and the time (in seconds) of the first occurrence of irritating vascular phenomena was monitored for 300 seconds.
The test was based on the observation of the following phenomena: vasoconstriction (VAS), haemorrhage (HEM) and coagulation (COA). The positive control was done with a NaOH solution (0.1 M) (n=6) and a sodium lauryl sulfate solution (0.1%, w/v) (n=6) and the negative control with NaCl (0.9%, w/v) (n=6). The irritation score (IS) was determined by Eq. 1:

Eq. (1): IS = 5x (301-HEM time) / 300 + 5x (301-VAS time)/ 300 + 5x (301-COA time) / 300

The irritating phenomena were classified according to the IS, as non-irritating (0-0.9), slightly irritating (1-4.9), moderately irritating (5-8.9) and extremely irritating (9-21) (27).

Washability profile using porcine ear skin

The samples (HG-$NC_{A+R+TiM}$ and HG-FREE) were subjected to washability measures using a modified Franz diffusion cell. The porcine skin was kept between the donor and recipient chambers of a Franz cell. In the donor chamber, a flow of PBS buffer (pH 7.4) was perfused. The flow was adjusted to 3 mL/min with a pump and the PBS buffer was collected at predetermined times and the avobenzone quantified by HPLC. The same buffer was used as the receptor medium, and the system was maintained at 37 °C. Each sample (200 mg) was spread on the pig's skin surface, without any washing for 30 minutes, to allow the hydrogels to adhere to the skin. After that period, the pump was turned on and the flow of buffer over the sample simulated the action of formulation removal (28).
After the washability experiments, the pig ear skin membranes were subjected to extraction, where they were perforated and put in contact with the extracting solution (mobile phase - avobenzone), vortex 2 min and sonication for 30 min, then the samples were filtered (0.45 µm) and quantified by HPLC. In addition, the excess sample that was not washed during the experiment period and the receptor medium that was in contact with the porcine membrane was collected, filtered, and quantified by HPLC.

Evaluation *in vitro* effectiveness of formulations

In order to evaluate the in vitro effectiveness of the developed formulations, we observe the performance of each sample against UV light absorption. The samples were added to a quartz cuvette (model 106Q-S, Hellma, Germany), with a capacity of 2.6 µL and an optical path length of 0.01 mm arranged by a support (model 013.000, Hellma, Germany). The scan was performed between wavelengths 280-400 nm in a spectrophotometer (Shimadzu UV-1800), the baseline was previously zeroed with HG-B (29).
Hydrogels composed from LNC suspensions (LNC-B; LNC-AVO and LNC-AVO+RSV) were also evaluated. In addition, for comparative purposes, a solution of avobenzone in capric/caprylic triglycerides at a concentration of 2.5 mg/mL was prepared to verify the absorption of the organic sunscreen in solution.

Statistical analysis

The results are expressed as mean ± standard deviations. Statistical data analysis was performed using Analysis of Variance (ANOVA) for one factor: Anova “One-way”, followed by the Tukey test for multiple groups ($p \leq 0.05$).

Results

Identification of microalgae

The microalgae (species *Scenedesmus ecornis*) were collected, isolated, and identified with the aid of an optical microscope (Figure 1). In relation to morphological characteristics, they presented from two to four flat cells arranged in colonies (30).

Characterization of nanocapsule suspensions

The formulations (LNC-B, LNC-AVO and LNC-AVO+RSV) presented unimodal particle size distribution in the nanometric range (Figure 2A) based on the volume (d [4.3]), close to 220 nm. Among the formulations, the radar chart indicates characteristics of unimodal size distributions and the absence of micrometric particles

(Figure 2B). For all formulations, the average particle diameter values obtained from the dynamic light scattering technique were close to 205 nm, with a unimodal population. The zeta potential values ranged from -9.0 to -11 mV and the PDI values were less than 0.1. The span values were below 1.7 for all formulations.

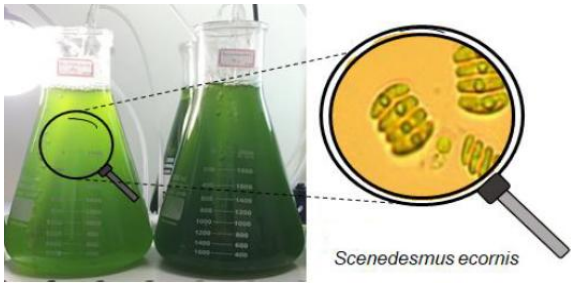

Figure 1. Cultivation of microalgae *Scenedesmus ecornis* used as drying support.

The pH measurements showed that the formulations had slightly acidic characteristics, approximately 5.2 ± 0.03. The avobenzone content in the formulations were 2.50 ± 0.04 mg/mL for LNC-AVO and 2.50 ± 0.05 mg/mL for LNC-AVO+RSV, the resveratrol content was 0.10 ± 0.00 mg/mL. The encapsulation efficiency values for avobenzone and resveratrol were 100% and 99% for LNC-AVO and LNC-AVO+RSV, respectively. Avobenzone was not detected in any of the ultrafiltrates.

Characterization of spray-dried nanocapsules

The nanosuspensions dried with titanium dioxide visually showed a white color and homogeneous appearance. Additionally, the dried formulations with titanium dioxide and microalgae resulted in a fine powder of light green color and homogeneous appearance. The process yields were 69.8 ± 3.1% and 67.4 ± 0.5% for LNC-AVO and LNC-AVO+ RSV, respectively, dried with titanium dioxide; 70.6 ± 1.9% and 70.73 ± 1.7% for LNC-AVO and LNC-AVO+RSV dried with titanium dioxide and microalgae, respectively. Moisture content was low (<2.0%) and the powders presented contents near to the expected concentrations (Table 1).

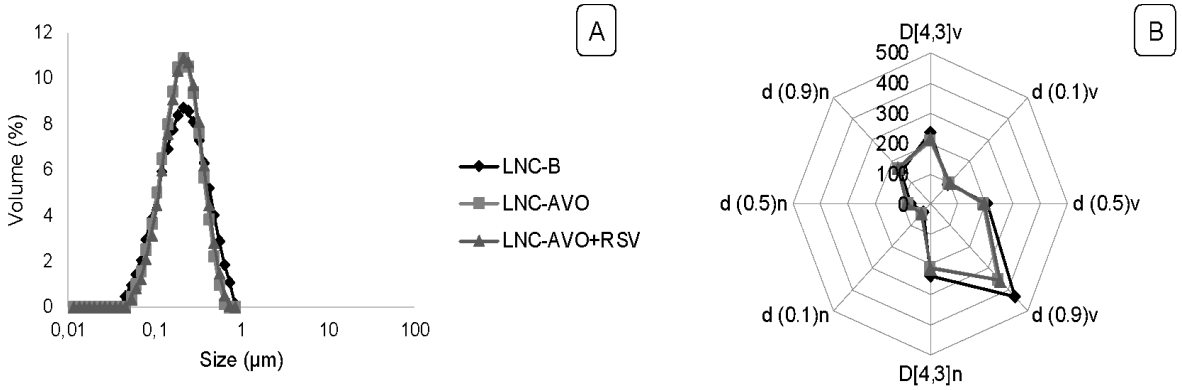

Figure 2. Particle size distributions by laser diffraction. A: volume (%) x size (µm); B: radar chart.

Table 1. Physicochemical characteristics of powders.

		D [4.3] µm (Refractive Index.)		Drug content (mg/g)	
Formulation	Moisture content (%)	PCL	TiO_2	Avobenzone	Resveratrol
LNC-AVO_{TiO2}	1.50 ± 0.03	47.5 ± 11.0	38.60 ± 7.70	35.70 ± 0.06	-
LNC-AVO_{TiO2+M}	1.50 ± 0.01	67.9 ± 10.0	60.90 ± 2.71	35.40 ± 0.45	-
LNC-AVO+RSV_{TiO2}	1.60 ± 0.21	64.2 ± 15.0	51.50 ± 1.42	35.70 ± 1.07	1.30 ± 0.00
LNC-AVO+RSV_{TiO2+M}	1.50 ± 0.10	68.4 ± 11.0	52.10 ± 7.95	35.80 ± 0.31	1.30 ± 0.02

The results are expressed as means and standard deviations. LNC-AVO_{TiO2}: lipid-core nanocapsules containing avobenzone spray-dried using only titanium dioxide, LNC-AVO_{TiO2+M}: lipid-core nanocapsules containing avobenzone spray-dried using titanium dioxide and microalgae, LNC-AVO+RSV_{TiO2}: lipid-core nanocapsules containing avobenzone and resveratrol spray-dried using only titanium dioxide, LNC-AVO+RSV_{TiO2+M}: lipid-core nanocapsules containing avobenzone and resveratrol spray-dried using titanium dioxide and microalgae.

The formulations of nanocapsules (LNC-AVO and LNC-AVO+RSV) dried with titanium dioxide presented a nanometric and micrometric distribution profiles considering the PCL refractive index (Figure 3A). However, for samples dried with titanium dioxide and microalgae, using the PCL refractive index, only the micrometric profile was observed. In Figure 3B, all samples characterized from the TiO_2 refractive index indicated the particle diameter in the micrometric size range.

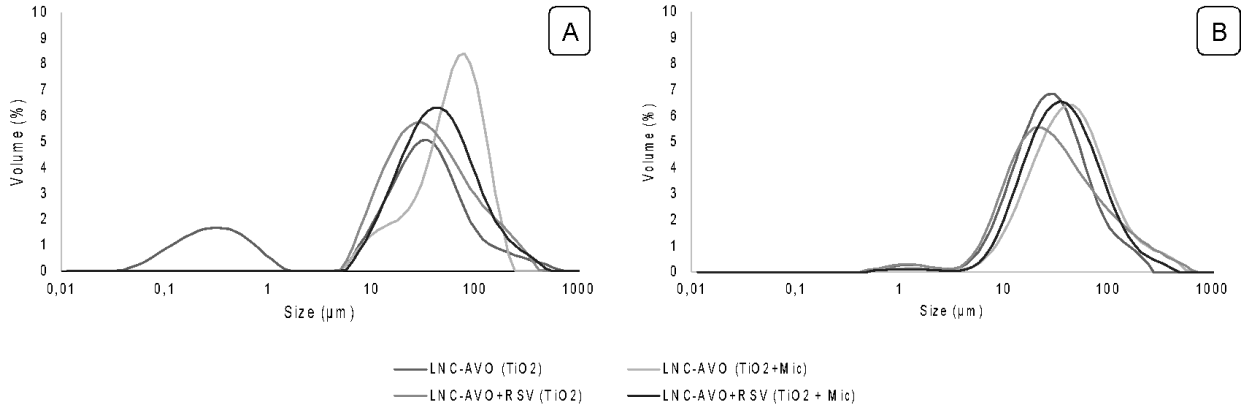

Figure 3. Particle size distribution profiles of the formulations obtained by laser diffraction. A: PCL refractive index; B: TiO_2 refractive index.

Figure 4 shows the morphological aspects of the spray-dried powders. All powders presented similar microparticles with exception of the microalgae sample. Microalgae structure (*Scenedesmus ecornis*) is smooth and with cell clusters (Figure 4A). Particles of the LNC-AVO_{TiO2} formulation exhibited an irregular surface (Figure 4B). LNC-AVO_{TiO2+M} formulation presented clusters of particles with irregular shape (Figure 4C). LNC-AVO+RSV_{TiO2} formulation showed the presence of rough surface clusters (Figure 4D). LNC-AVO+RSV_{TiO2+M} presented microparticles with irregular surface (Figure 4E).

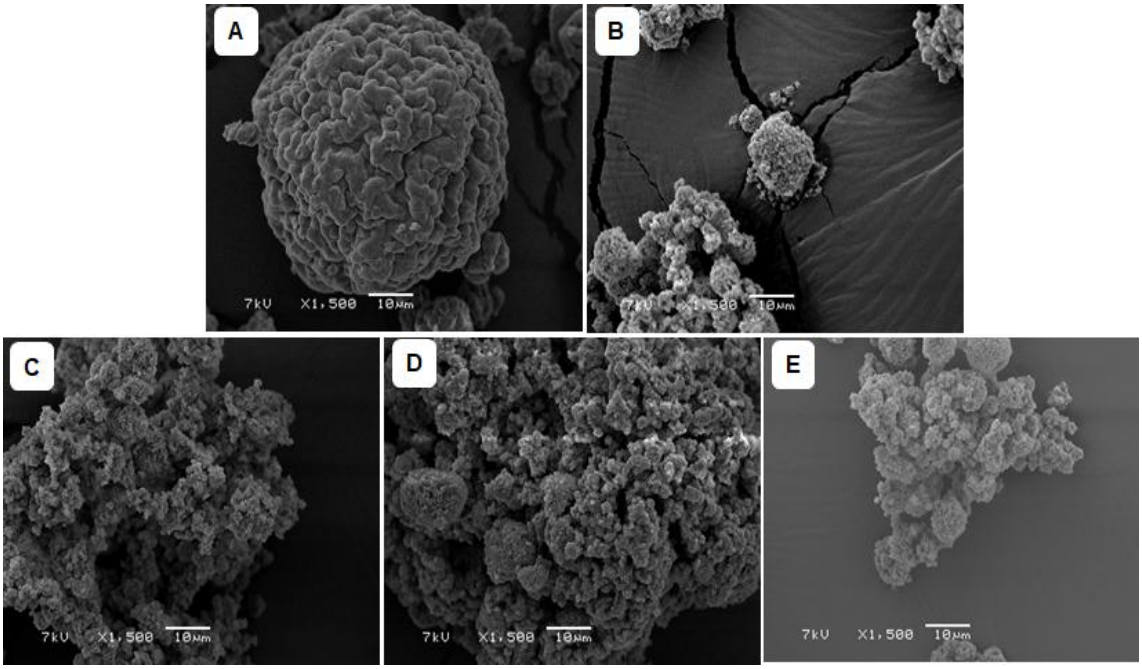

Figure 4. SEM images of particles. (A) Microalgae; (B) lipid-core nanocapsules containing avobenzone spray-dried using only titanium dioxide (LNC-AVO_{TiO2}); (C) lipid-core nanocapsules containing avobenzone spray-dried using titanium dioxide and microalgae (LNC-AVO_{TiO2+M}); (D) lipid-core nanocapsules containing avobenzone and resveratrol spray-dried using only titanium dioxide (LNC-AVO+RSV_{TiO2}) and (E) lipid-core nanocapsules containing avobenzone and resveratrol spray-dried using titanium dioxide and microalgae (LNC-AVO+RSV_{TiO2+M}).

Development and characterization of hydrogels

Particle diameter

The HG-NC$_{A+R+TiM}$ was characterized for particle diameter by laser diffraction, considering the PCL and TiO2 refractive index based on the volume value (d [4.3]), obtaining values of 11 ± 2.55 µm and 16 ± 5.47 µm with a span value of 4.18 ± 1.12 and 2.84 ± 1.50, respectively, after 5 minutes of agitation. The hydrogels volume distribution profile showed a micrometric peak, with the presence of a nanometric population, while the distribution by number showed only the nanometric profile (Figure 5).

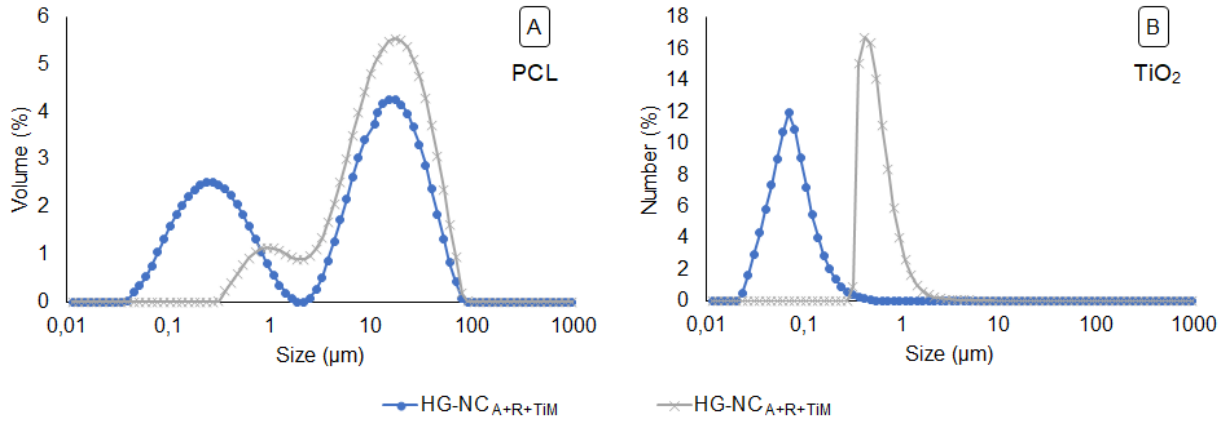

Figure 5. Particle size distribution of the hydrogels obtained by laser diffraction using PCL and TiO_2 as refractive index. (A) volume and (B) number.
(Blue) HG-NC$_{A+R+TiM}$ and (Gray) HG-NC$_{A+R+TiM}$

Visual and morphological characterization

The HG-NC$_{A+R+TiM}$ showed a bright and homogeneous appearance with a light green color. On the other hand, the free hydrogel (HG-FREE) had a homogeneous appearance and white color. Although the blank hydrogel (HG-B), composed exclusively of Lecigel®, preservative and water mixture, was homogeneous, colorless, and transparent. The morphological analysis of the hydrogels showed that HG-B forms a transparent film on the carbon tape (Figure 6A), while HG-FREE presented small clusters of particles (Figure 6B) and, finally, HG-NC$_{A+R+TiM}$ forms a film constituted of nano- and microparticle aggregates (Figure 6C).

Avobenzone and resveratrol quantifications and pH of the hydrogels

The formulations (HG-NC$_{A+R+TiM}$ and HG-FREE) presented content close to the expected theoretical values, 1.40 and 0.05 mg/g for avobenzone and resveratrol, respectively (Table 2). In percentage terms, the avobenzone and resveratrol contents were above 80%. The pH for all the hydrogels were close to neutrality, 7.1 for the HG-B, 7.2 for the HG-FREE, and 7.52 for the HG-NC$_{A+R+TiM}$.

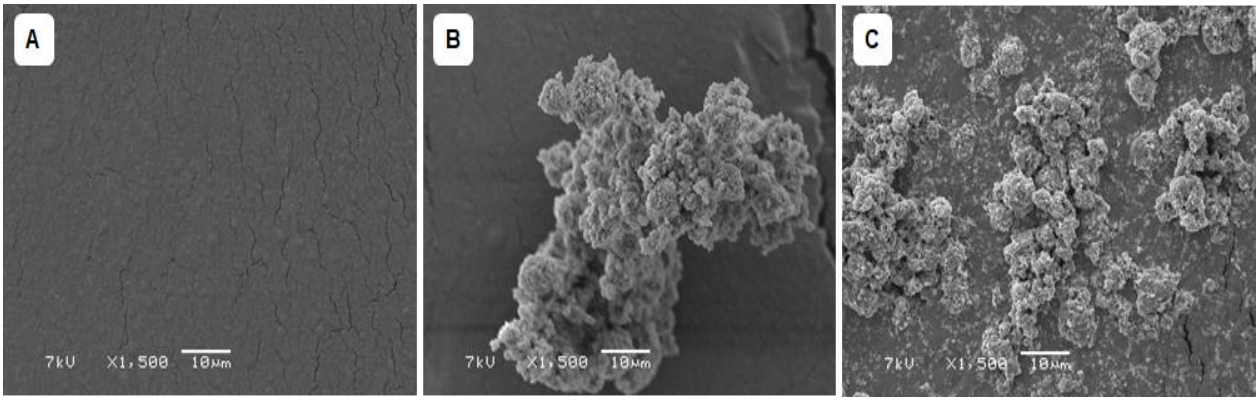

Figure 6. SEM images of hydrogels. (A) Blank hydrogel (HG-B); (B) hydrogel containing free avobenzone and resveratrol dispersed with polymer in water (HG-FREE) and (C) hydrogel containing spray-dried avobenzone and resveratrol nanocapsules using titanium dioxide and microalgae as the drying adjuvant (HG-NC$_{A+R+TiM}$).

Table 2. Content and pH of the hydrogels (HG-B; HG-FREE and HG-$NC_{A+R+TiM}$ (n=3)).

Hydrogels	Drug content (%)		Drug content (mg/g)		pH
	AVO	RSV	AVO	RSV	
HG-B	*	*	*	*	7.1 ± 0.16
HG-FREE	95.12 ± 0.10	95.08 ± 0.91	1.34 ± 0.03	0.05 ± 0.11	7.2 ± 0.33
HG-$NC_{A+R+TiM}$	88.57 ± 0.03	80.56 ± 0.02	1.24 ± 0.04	0.04 ± 0.12	7.5 ± 0.23

The results are expressed as means and standard deviations. (*****) It is not quantifiable. AVO: avobenzone; RSV: resveratrol.

Rheological behavior

In this work, the rheological profiles of the hydrogels (HG-B and HG-$NC_{A+R+TiM}$) were evaluated according to the determination coefficients (r^2) obtained from shear stress curves versus shear rate (Figure 7). In Table 3, the determination coefficients are presented with the standard deviation, considering the four models: Casson, Bingham, Ostwald and Herschel-Bulkley. The Ostwald model was the one that obtained the highest determination coefficient for HG-B and HG-$NC_{A+R+TiM}$ with values of 0.9903 ± 0.0025 and 0.9944 ± 0.0029, respectively. The flow indexes (n) obtained were less than 1, being in accordance with the properties of pseudoplastic flows (Table 4). The consistency indexes (K) showed significant differences ($p \leq 0.05$) between the HG-B and HG-$NC_{A+R+TiM}$, with a smaller consistency of HG-$NC_{A+R+TiM}$ compared to HG-B.

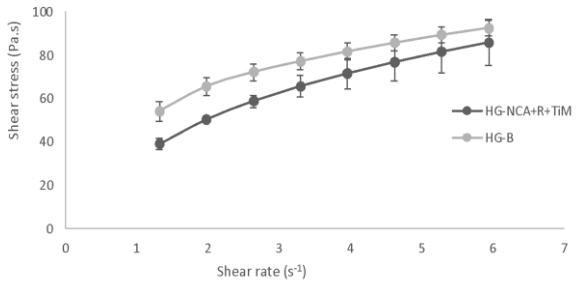

Figure 7. Rheogram of the shear rate (s-1) versus shear stress (Pa.s) of HG-B (blank hydrogel) and HG-$NC_{A+R+TiM}$ (hydrogel containing spray-dried avobenzone and resveratrol nanocapsules using titanium dioxide and microalgae as the drying adjuvant).

Table 3. Determination coefficients (r2) for different flow models, obtained to describe the rheological profiles of hydrogel containing spray-dried avobenzone and resveratrol nanocapsules using titanium dioxide and microalgae as drying adjuvant (HG-$NC_{A+R+TiM}$) and blank hydrogel (HG-B).

Models	Hydrogels	
	HG-B	HG-$NC_{A+R+TiM}$
Bingham	0.9536 ± 0,0027	0.9727 ± 0.0015
Casson	0.9748 ± 0,0030	0.9853 ± 0.0025
Ostwald	**0.9903 ± 0.0025**	**0.9944 ± 0.0029**
Herschel-Bulkley	0.8997 ± 0,0066	0.9473 ± 0.0095

Table 4. Flow indexes (n) and consistency (K) of the hydrogels.

Hydrogels	N	K
HG-B	0.35 ± 0.03	48.26 ± 2.31*
HG-$NC_{A+R+TiM}$	0.51 ± 0.13	34.22 ± 3.77**

Statistical difference between the indexes (*) and (**) $p \leq 0.05$. HG-B: blank hydrogel; HG-$NC_{A+R+TiM}$: hydrogel containing spray-dried avobenzone and resveratrol nanocapsules using titanium dioxide and microalgae as the drying adjuvant and blank hydrogels.

Skin permeation/penetration of avobenzone

To determine the permeation/penetration of avobenzone from hydrogels (HG-FREE and HG-$NC_{A+R+TiM}$), Franz diffusion cells were used. After 24h of experiment, avobenzone was not detected in the receptor compartment. In both experiments, the same amount of avobenzone (280 µg/cm^2) contained into hydrogels was applied on the skin surface. A high concentration of avobenzone was retained on the skin surface, indicating a significant difference in the amounts of UV filter, for the HG-FREE (272.17 ± 19.88 µg/cm^2) and the HG-$NC_{A+R+TiM}$ (266.78 ± 16.59 µg/cm^2). The results are shown in Figure 8 and are expressed as concentration of avobenzone retained in the different skin viable layers.

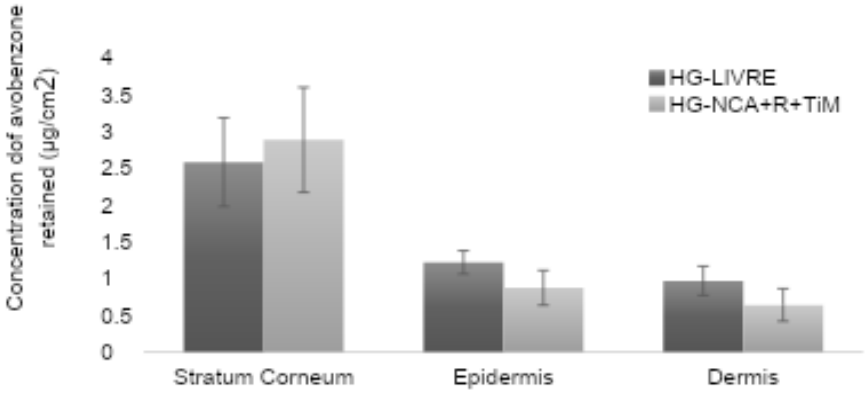

Figure 8. Skin penetration of avobenzone from hydrogel containing spray-dried avobenzone and resveratrol nanocapsules using titanium dioxide and microalgae as the drying adjuvant (HG-$NC_{A+R+TiM}$) and hydrogel containing free avobenzone and resveratrol dispersed with polymer in water (HG-FREE) in the porcine skin viable layers. Values represent mean ± standard deviation (n=3) *$p \leq 0.05$.

The highest concentration of avobenzone was found in the stratum corneum, but no significant differences between hydrogels ($p \geq 0.05$) were found. However, for epidermis and dermis, decreases in the concentration of avobenzone for both hydrogels were observed. Although, avobenzone from HG-FREE was more retained in the epidermis (1.22 ± 0.24 µg/cm2) when compared to HG-$NC_{A+R+TiM}$ (0.87 ± 0.16 µg/cm2) ($p \leq 0.05$). Likewise, a significant amount of avobenzone was retained in the dermis from HG-FREE (0.97 ± 0.22 µg/cm^2) when compared to HG-$NC_{A+R+TiM}$ (0.64 ± 0.20 µg/cm^2) ($p \leq 0.05$).

Evaluation of the irritation potential

Table 5 describes the scores of the substances and hydrogels analyzed in this study. As expected, the positive control with sodium hydroxide (0.1M) was classified as extremely irritating 12.99 ± 0.5 (IS value above ≥ 9). On the other hand, the positive control with sodium lauryl sulfate (1.0% w/v) was slightly irritating 2.65 ± 0.9 (IS value ≤ 4.9). For negative control with saline solution (0.9% w/v), irritation reactions were not observed. The hydrogels studied were classified as non-irritating (IS of zero).

Figure 9 shows images of the control groups and hydrogels applied on the chorioallantoic membrane. It is evident that there are no changes of the chorioallantoic membrane when in contact with hydrogels (HG-B, HG-FREE and HG-$NC_{A+R+TiM}$) for 300 seconds, when compared to the two positive control groups (sodium lauryl sulfate and sodium hydroxide). The endpoints of irritancy (hemorrhage and coagulation) were observed in the positive control group with sodium hydroxide, while in the positive control group with sodium lauryl sulfate vasoconstriction was detected, indicating minor irritant potential.

Table 5. Classification of results obtained regarding the irritating potential of the substances and hydrogels (HG-B, HG-FREE and HG-$NC_{A+R+TiM}$) performed using the HET-CAM test.

Groups	IS	Classification
NaOH	12,99 ± 0,5	Extremely irritating
Sodium lauryl sulfate	2,65 ± 0,9	Slightly irritating
Saline solution	0 ± 0	Non-irritating
HG-B	0 ± 0	Non-irritating
HG-FREE	0 ± 0	Non-irritating
HG-$NC_{A+R+TiM}$	0 ± 0	Non-irritating

Classification: Non-irritating (0 – 0,9), slightly irritating (1 – 4,9), moderately irritating (5 – 8,9) and extremely irritating (9 - 21). (27).

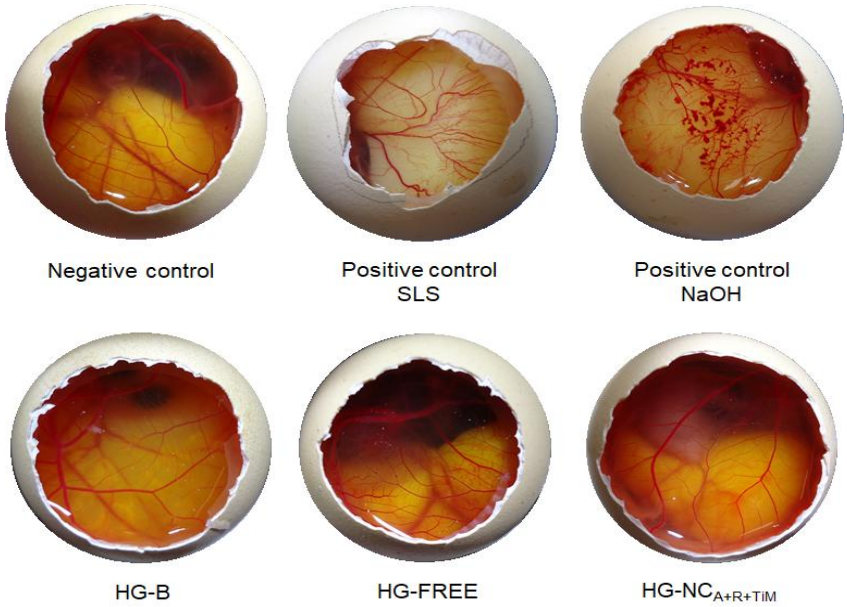

Figure 9. Images of chorioallantoic membrane reactions caused after the application of different substances and hydrogels for 300 seconds. LSL: sodium lauryl sulfate; NaOH: sodium hydroxide; HG-B: blank hydrogel; HG-FREE: hydrogel containing free avobenzone and resveratrol dispersed with polymer in water; HG-NC$_{A+R+TiM}$: hydrogel containing spray-dried avobenzone and resveratrol nanocapsules using titanium dioxide and microalgae as the drying adjuvant.

Washability profile

Initially, it was observed that HG-NC$_{A+R+TiM}$ was strongly adhered to the pig's ear skin surface compared to HG-FREE. This was confirmed by quantification of the accumulated washed avobenzone, which was significantly different between hydrogels ($p \leq 0.05$). The results are shown in Figure 10 and are expressed as the accumulated amount of avobenzone washed as a function of time. At the end of 300 minutes, the accumulated amount of avobenzone for HG-FREE was 79.88 ± 4.53 µg, corresponding to 60.06 ± 3.41% of the applied formulation. In contrast, HG-NC$_{A+R+TiM}$ strongly resisted the washing flow with only 15.50 ± 4.45 µg accumulated avobenzone at the end of the experiment; in percentage terms this is equivalent to 11.65 ± 3.35% of applied formulation.

The results indicated that both hydrogels did not allow the permeation of avobenzone through the skin, considering that the UV filter was not detected in the receptor medium. However, the amount of avobenzone adsorbed on the skin was significantly higher ($p \leq 0.05$) for HG-NC$_{A+R+TiM}$ (77.59 ± 22.25 µg) comparing with the HG-FREE (10.25 ± 2.93 µg).

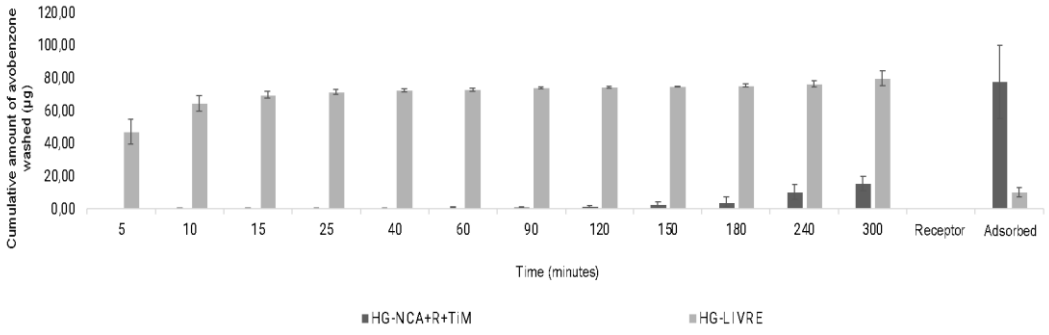

Figure 10. Washability profile of hydrogels from the cumulative amount of avobenzone (µg) as a function of time (minutes). Values represent mean ± standard deviation (n=3). Statistical analysis: One-way ANOVA followed by post hoc comparisons (Tukey Test) ($p<0.05$). HG-FREE: hydrogel containing free avobenzone and resveratrol dispersed with polymer in water; HG-NC$_{A+R+TiM}$: hydrogel containing spray-dried avobenzone and resveratrol nanocapsules using titanium dioxide and microalgae as the drying adjuvant.

Evaluation *in vitro* effectiveness

This essay showed progressive increases in effectiveness as the complexity of the formulations increased in terms of composition: CCT$_A$, HG-LNC$_B$, HG-LNC$_{A+R}$, HG-NC$_{B+Ti}$, HG-NC$_{A+Ti}$, HG-NC$_{A+TiM}$, HG-NC$_{A+R+Ti}$ and HG-NC$_{A+R+TiM}$ (Figure 11).

The HG-NC$_{A+R+TiM}$ absorbed more UV light with maximum wavelengths between 305 and 328 presenting intensities of 0.745 and 0.773, respectively. Our

observations highlight that hydrogels produced from the incorporation of spray-dried powders increase the absorption of UV light.

In addition, it was observed that the dispersion of avobenzone prepared in capric/ caprylic triglycerides was able to absorb UV light with wavelengths between 346 and 358 nm, but with a low intensity of 0.034 and 0.042. The hydrogel produced from lipid-core nanocapsules suspension of avobenzone and resveratrol (HG-LNC_{A+R}), absorbed the UV light with bigger intensity and maximum wavelengths between 362 and 365, compared to the hydrogel that contained blank lipid-core nanocapsules suspensions.

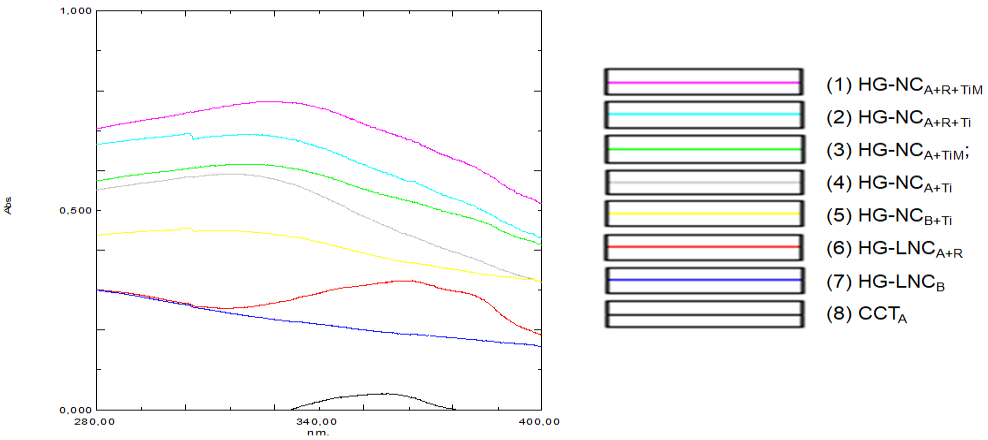

Figure 11. UV spectrum: Comparison between the complexity of hydrogels. (1) HG-$NC_{A+R+TiM}$: hydrogel containing spray-dried avobenzone and resveratrol nanocapsules using titanium dioxide and microalgae as the drying adjuvant; (2) HG-NC_{A+R+Ti}: hydrogel containing spray-dried avobenzone and resveratrol nanocapsules using only titanium dioxide as the drying adjuvant; (3) HG-NC_{A+TiM}: hydrogel containing spray-dried avobenzone nanocapsules using titanium dioxide and microalgae as the drying adjuvant; (4) HG-NC_{A+Ti}: hydrogel containing spray-dried avobenzone nanocapsules using only titanium dioxide as the drying adjuvant; (5) HG-NC_{B+Ti}: hydrogel containing spray-dried blank nanocapsules using only titanium dioxide as the drying adjuvant; (6) HG-LNC_{A+R}: hydrogel containing lipid-core nanocapsules suspension of avobenzone and resveratrol; (7) HG-$LNC_{B:}$ hydrogel containing blank lipid-core nanocapsules suspensions; (8) CCT_A: caprylic/capric triglycerides containing free avobenzone.

Discussion

The variety of cosmetic formulations using biocompounds or microalgal extracts is increasing (31). Microalgae can adapt themselves to physical and chemical variations, which allows better growing conditions. In addition, most of these microorganisms have characteristics that facilitate their taxonomy (32). The species *Scenedesmus ecornis* has from two to eight flat cells, but this number can vary from eight to sixteen colonies due to the environmental conditions of the place where it is found (33). Similar morphologic characteristics (presented from two to four flat cells arranged in colonies) were found in this work through microscopic analysis, corroborating with the literature.

A high content of fatty acids has been previously described in this species as well as its antioxidant activity (18). In this work, the species *Scenedesmus ecornis* was used as a drying support, to reducing UV light skin damage. Indeed it has already been described by Ariede and collaborators (2017) that microalgae develop efficient protective systems against oxygen reactive species and free radicals, highlighting an increase in the production of both chlorophyll and mycosporine, that can act in cosmetics against the harmful effects of UV radiation (19).

The lipid core nanocapsules developed (LNC-B, LNC-AVO and LNC-AVO+RSV) showed average diameters in the nanometer range of 210, 214 and 220 nm, respectively, corroborating results previously obtained by our research group, which used the interfacial polymer deposition method to prepare nanoparticles containing benzophenone (29, 34) and resveratrol (11). For all suspensions, the zeta potential negative values can be explained by the presence of polysorbate 80 and PCL in the formulations (21). The slightly acidic pH characteristic is attributed to the constituents of the formulation and is suitable for topical application due to its similarity to the pH of the skin (35).

The radar chart expressed the data of average particle size distribution (d [4,3]) and diameters at the $d_{0,1}$, $d_{0,5}$ e $d_{0,9}$ percentiles represented by the volume and number measurements of the laser diffraction technique. From this, it is possible to determine the fingerprints of the formulations in pre-formulation studies. Our results indicated that all the nanosuspensions had d(0.9)v lower than 500 nm and d(0.5)n lower than 200 nm, confirming the narrow polydispersion of the system (PDI < 0.1) and homogeneous (span <1.7), according to the characteristics of polymeric nanocapsules described by Bianchin and collaborators (2015) (36).

The drug content and encapsulation efficiency of avobenzone and resveratrol in the nanocapsules (LNC-

AVO and LNC-AVO-RSV) were close to the expected values. The high recovery confirmed a complete extraction of both substances. Due to the high lipophilicity of avobenzone and the hydrophobic character of resveratrol, this result can be explained by the probable interactions between organic groups (for example: C=O of avobenzone and -OH of resveratrol) with the oily core of particle. Furthermore, the avobenzone was not detected in any of the ultrafiltrates due to its low solubility in water, 0.01 mg/L (20ºC) (37). The distribution of the drug in aqueous dispersions of lipid-core nanocapsules was classified according to the physical parameter *log* D. Given this, avobenzone, which has *log* D 4.51, falls into type VI, and would be present in the core of the nanoparticles. On the other hand, resveratrol has *log* D equal to 3.1, indicating that the active substance would be more concentrated in the polymeric wall (38).

Drying nanoparticle suspensions improves their physicochemical stability, providing versatile products that can be converted into various pharmaceutical forms (39).

Therefore, we produced five different powders by spray drying using titanium dioxide and/or a mixture of it with the microalgae to lower the risk of microbiological contamination. Generally, the yield variation in the drying process is related to the formulation characteristics versus the type of adjuvant used (13). Lactose (water-soluble excipient) spray-dried nanocapsules containing tretinoin showed a yield close to 80% (43). In contrast, curcumin-loaded lipid-core nanocapsules dried with the aid of a blend of maltodextrin and L-leucine (90:10 w/w) showed a yield around 70% (40). In the present work, the yield of the powders in the drying process was above 69%. These results can be explained by the tendency of some particles to stick to the surface of the drying tower (44).

The avobenzone and resveratrol contents in the spray-dried powders were above 85%, so despite the drying temperature of 120ºC, there was no significant loss of these substances. Marchiori et collaborators (2014) obtained a 95% tretinoin content after drying nanoemulsions with lactose, discarding the hypothesis of a thermal degradation (41).

The type of drying adjuvant and the characteristics of the nanostructures are parameters that influence the recovery of the nanometric profile of lipid-core nanocapsules. The particle size distributions were determined by considering the PCL and titanium dioxide refractive index. The formulations dried using only TiO_2 and evaluated for PCL refractive index showed two populations (nanometric and micrometric particle agglomerates). In contrast, in the formulations dried with titanium dioxide and microalgae, evaluated for PCL refractive index, only the micrometric profile was observed, due to the presence of a micrometric support (the microalgae). The particles are supposably covering the microalgae. The particle diameter of all formulations characterized for the TiO_2 refractive index, indicated micrometric population.

The morphological analysis showed significant differences in the microalgae spray-dried powders structure compared to LNC-AVO_{TiO2}, LNC-AVO_{TiO2+M}, LNC-AVO+RSV_{TiO2} and LNC-AVO+RSV_{TiO2+M}. The tendency to form robust microparticles agglomerates with irregular surfaces was observed in all powders dried with titanium dioxide, with characteristics of amorphous substances, as observed by Lewicka and collaborators (2011) (42). During the spray drying process, it is extremely complicated to control the agglomeration of particles, which occurs due to the interaction between the variables of the equipment itself, such as atomization process, the mixing of spray and hot air and the deposition of dry material being introduced into the drying chamber (43). Despite being freeze-dried to preserve cell composition, prolong viability, and reduce sample deterioration, smooth-surfaced cell clusters were present in the microalgae structure.

Other approaches to convert nanocapsules into solid products by spray drying using hydrophobic or hydrophilic excipients as drying adjuvants have been reported. Müller and collaborators (2000) used colloidal silicon dioxide as a drying adjuvant for PCL and Eudragit S90® polymeric nanocapsules containing diclofenac. The morphological analysis of the powders surface showed that the nanocapsules morphology remained intact and no change in particle size (close to 200 nm) was detected after the spray drying process (15). In our work, although titanium dioxide is a water-insoluble substance, the morphological analysis of the powders surface showed a tendency to agglomerate and precipitate because of its high density (42).

The silicon dioxide was used at a concentration of 3% (w/v) by Schaffazick and collaborators (2003) as a drying adjuvant for melatonin nanocapsules, the morphological analysis by SEM showed spherical-shaped microparticles with a narrow diameter distribution (70). On the other hand, when we use titanium dioxide in the same concentration mentioned by Schaffazick and collaborators (2003), clusters of particles were observed. However, titanium dioxide was chosen as an adjuvant because of its widespread use as an inorganic sunscreen.

For formulations containing sunscreens, it is essential that the particles covering the stratum corneum have an occlusive effect on the skin and prevent the UV rays' action without penetrating the other skin layers. Given this, the HG-$NC_{A+R+TiM}$, particle diameter was characterized by laser diffraction, considering the PCL and TiO_2 refractive index based on the volume value (d [4,3]) and in terms of particle number. Remarkably, the average volume distribution of HG-$NC_{A+R+TiM}$ showed a bimodal profile with higher polydispersity.

Cardoso and collaborators (2019) characterized chitosan hydrogels containing nanoencapsulated phenytoin and observed that all hydrogels showed particle size distribution by volume in the micrometric and nanometric size. However, considering the number-weighted size distribution, a similar particle size

distribution was observed for all hydrogels compared to their respective original suspensions (43). The findings of this work are in accord with our results.

Although the mean size of LNC-AVO+RSV$_{TiO2+M}$ is larger before inclusion in the hydrogel, this difficulty can be overcome by simultaneous drying with nanocapsules, considering that we obtained a product (HG-NC$_{A+R+TiM}$) that redisperses. This feature had been previously reported by Contri and collaborators (2014), who evaluated the particle size distribution of chitosan hydrogels containing polymeric nanocapsules, considering the refractive index of Eudragit® RS 100. After the analyses, they concluded that nanoparticle aggregation can occur in the hydrogel network accompanied or not by the formation of micrometric chitosan structures (45).

In order to evaluate the influence of incorporation of spray-dried powders into Lecigel® (sodium acrylates copolymer and lecithin), HG-NC$_{A+R+TiM}$ was produced and compared with HG-FREE and HG-B. Lecigel® is a gelling agent with emulsifying property used to increase the viscosity and stability of formulations. In addition, it provides the "phospholipid touch", characterized by a cool, smooth, and silky skin feel, improving skin hydration and bioavailability of actives (46). The scanning electron microscopy analysis evidenced the differences between the hydrogels researched, highlighting HG-FREE, with small agglomerates of amorphous particles (42).

In percentage terms, the avobenzone and resveratrol contents in the hydrogels (HG-NC$_{A+R+TiM}$ and HG-FREE) were above 80%. All hydrogels showed similar pH values, close to neutrality. However, the pH values of the hydrogels, when compared to the suspensions, were higher. Lecithin, a heterogeneous mixture of phospholipids, is one of the main components of Lecigel® with pH around 7 (46). Complementarily, TiO_2 has a pH of 7.5 (47) and is one of the main components of HG-NC$_{A+R+TiM.}$ The Lecigel® is stable over a wide range of pH (between 4 and 8) (48)

The analysis of the rheological properties of nanocapsules incorporated into semisolids for topical administration of drugs and/or cosmetics is essential to determine the technological potential of these systems, as it can influence the topical delivery of the substances and their subsequent bioavailability (49). Hydrogels can be prepared with natural, semi-synthetic and synthetic polymers (50). Examples of polymers used in the incorporation of nanosystems are chitosan (44, 45), hydroxyethyl cellulose (28, 51) and Carbopol® (52, 53)

The rheological profiles of the hydrogels (HG-B and HG-NC$_{A+R+TiM}$) showed coefficient of determination lower than 1, compatible with the description of the Ostwald model. This mathematical model describes the non-Newtonian behavior with pseudoplastic flow, i.e., no linear relationship was observed between shear stress and shear velocity (50, 54). This, in turn, is suitable in topical products, as it ensures uniform distribution when spread on the skin (55). The flow rates (n) obtained corroborate the rheological profile discussed above (54). This rheological property is desirable because it describes a formulation with a suitable flow characteristic for dermal application (56). The consistency indices (K) showed significant differences between HG-B and HG-NC$_{A+R+TiM}$ ($p \leq 0,05$), with lower consistency of HG-NC$_{A+R+TiM}$ compared to HG-B. This difference can be attributed to the fact of a greater interaction between the gelling polymer (Lecigel®) and water, without the presence of the other constituents.

Hydrogels are cross-linked polymeric networks prepared from hydrophilic polymers, which can absorb and retain a high-water content while maintaining their three-dimensional integrity (56). Most of the published work develops hydrogels replacing water by direct incorporation of nanosuspensions. Zuglianello and collaborators (2018) produced hydrogels containing spray-dried tretinoin lipid-core nanocapsules and compared them to hydrogels that were produced with the original nanocapsule suspension (57). Their results indicated that the formulations exhibited identical rheological profiles. The Herschel-Bulkley model fitted the rheological profiles of both formulations. This model represents a pseudoplastic flux with yield stress. Thus, they highlighted the potential of spray-dried powders as intermediate products for the development of hydrogels (43). Our studies corroborate this application for powders.

Terroso and collaborators (2009) characterized the rheological properties of hydrogels containing spray-dried coenzyme Q10 nanocapsules and observed pseudoplastic flow (Ostwald model), consonant with our results. On the other hand, the formulation of hydrogels prepared from the nanosuspensions showed pseudoplastic flow with yield stress (Herschel-Bulkley model). This lack of agreement between the results was justified by the differences in Carbopol® concentration and to the type used in the different works (58).

Currently, *in vitro* models are widely used for skin penetration/permeation studies of substances. Indeed, they have numerous advantages and are relatively easy to perform and provide information about the interactions of formulations with the skin (59). The effectiveness of sunscreens is related to their ability to adhere to the skin, forming a protective film that prevents the action of UV radiation (59). After 24 hours of experiment, avobenzone did not permeate into the skin layers. Our results are in accordance with the legislation, which emphasizes that sunscreens should not reach the systemic circulation (60). The degree of sunscreen penetration through the skin depends mainly on the physicochemical properties of the formulation and the characteristics of the molecule itself (61). Regarding the viable layers of the skin, the highest concentration of avobenzone was found in the stratum corneum for the formulation of HG-NC$_{A+R+TiM}$, which validates the tendency for UV filters to become more adherent due to their high affinity for this layer.

Studies are constantly being conducted on the permeation/penetration of UV filters into the skin to

determine their safety (62). Therefore, several strategies are being adopted to minimize the possible absorption effects on the body, such as the use of colloidal carriers associated with final formulations (hydrogels, lotions, creams, and emulsions) to optimize topical application (4). In this context, we opted for the use of materials compatible with the hydrogel matrix, given the need for good adhesion to the most superficial layer of the skin.

Santos and collaborators (2014) developed hydrogels from polymeric nanoparticles containing octyl methoxycinnamate and compared them with hydrogels containing only the filter (64). The results showed a better retention of the filter in the stratum corneum for the nanotechnology-based hydrogels compared to the free form ones. Similarly, we identified greater retention in the stratum corneum for both studied hydrogels (HG-$NC_{A+R+TiM}$ and HG-FREE), but with significant differences in the penetration of avobenzone in the epidermis and the dermis. Thus, the nanotechnology-based hydrogel modulated the penetration of the filter into the layers of the skin.

Moreover, it is possible to say that the combination of avobenzone with titanium dioxide and microalgae in HG-$NC_{A+R+TiM}$ can help to decrease the penetration of the filter into the skin. Recently, the behavior of formulations containing sunscreens in the same combination of organic UV filters, avobenzone and octocrylene (Eusolex OCR), in free or microencapsulated form, was investigated and compared for evaluation in terms of penetration, retention on the skin surface and photostability. The analyses indicated that the encapsulated formulation showed a greater amount of the UV filters on the skin surface while in the traditional (free) formulation the filters penetrated significantly into the stratum corneum (65).

HET-CAM is an *in vitro* assay that was first described by Luepke (1985) (27) and is used to evaluate the irritation properties of a formulation on the vascular system (vasoconstriction, hemorrhage, and coagulation) when applied to the chorioallantoic membrane of embryonated hens' eggs on the tenth day of incubation. One of the advantages of this test is the possibility to evaluate different kinds of formulation, including insoluble substances, emulsions, gels, and solid particles (65). The HET-CAM assay is widely used for irritation evaluation because it is a rapid, sensitive, and inexpensive alternative to animal or human experiments. The analyzed hydrogels showed no irritant reactions on the chorioallantoic membrane. This was evident in the assay images after observation of the hydrogels, compared to the control groups.

The search for the development of safe and efficient photoprotective formulations is constant. In this sense, Barbosa and collaborators (2019) evaluated the irritant profile by HET-CAM of polymeric nanocapsules containing benzophenone. Based on the irritation scores of the control formulations, the components of the analyzed formulations were classified as non-irritating since no vascular events were observed during the 300 seconds (67). Regarding the influence of polymer surface charge, Contri and collaborators (2016) developed two types of nanocapsule suspensions, one cationic and the other anionic. They subsequently incorporated the cationic nanoparticles into chitosan gels and evaluated the irritant potential by HET-CAM, detecting no hemorrhage, lysis, or coagulation in any of the formulations (68). Our results are consonant with these previous studies.

In general, sunscreens should have good adhesion to the skin, forming a protective film against the sun's rays. The washability test was performed to evaluate the adhesion of the hydrogels to the skin, with HG-$NC_{A+R+TiM}$ standing out as strongly adhering to the skin surface in contrast to HG-FREE after 5h. In addition, HG-$NC_{A+R+TiM}$ was more resistant to wash flow. This behavior of HG-$NC_{A+R+TiM}$ is probably influenced by the association of the polymeric network of the hydrogel to the microparticles of the spay dried powders, with emphasis on the presence of TiO_2 (insoluble in water) and microalgae.

Furthermore, HG-$NC_{A+R+TiM}$ conferred resistance to the washing flow in PBS buffer, facilitating a sustained release of avobenzone and evidencing the adhesive capacity of this formulation, which ensures greater permanence of the UV filter on the surface in analogy to HG-FREE that was over-washed in the very first minutes.

Although the nature of UV filters plays an important role in their efficacy, carriers have had a key influence on the evolution of photoprotectors. Still, there are several factors to be addressed, such as instability and washability in water (55). When they are nanoencapsulated, lipophilic substances tend to be retained more on the skin surface, specifically in the stratum corneum. This is reflected in the amount permeated in the dermis and the receptor medium (69), corroborating our results. Chitosan hydrogels containing capsaicin (lipophilic amide) and dihydrocapsaicin nanocapsules showed low washing rate and prolonged adhesion on skin compared to hydroxyethyl cellulose hydrogels developed by Contri and collaborators (2013), demonstrating the adhesion ability of nanocapsules in controlling substance diffusion (28).

The nanoencapsulation of sunscreens is a viable option that significantly improves photoprotection. In order to evaluate the *in vitro* efficacy of formulations against UV light absorption, different hydrogels were produced from the direct incorporation of nanosuspensions and through the addition of spray-dried nanocapsules. Additionally, a dispersion of avobenzone in capric/caprylic triglycerides was prepared for comparative purposes. In our work, we can highlight HG-$NC_{A+R+TiM}$, which absorbed more UV light due to its more complex composition, showing a combined effect of absorption by the organic filter and the light scattered by the inorganic filter and the nanocapsules, with wavelength maxima between 305 and 328, showing intensities of 0.745 and 0.773, respectively.

Sunscreens should preferably absorb UV light in the wavelengths between 280-320 nm (70). Taking into consideration that HG-$NC_{A+R+TiM}$ obtained maximum wavelengths between 305 and 328, we can affirm its greater ability to absorb light at the erythematous wavelength compared to the other formulations (71). The composition of HG-$NC_{A+R+TiM}$ allowed a higher efficacy against UV light, which may be suggestive of higher protection when applied to the skin. Moreover, it was observed that the avobenzone dispersion prepared in capric/caprylic triglycerides was able to absorb UV light at wavelengths between 346 and 358 nm, but with low intensity 0.034 and 0.042. On the other hand, it is noteworthy that the hydrogel produced from LNC-AVO+RSV absorbed UV light with higher intensity, indicating that avobenzone is dissolved in the oil core of the nanocapsules with wavelength maxima between 362 and 365. It is worth noting that the hydrogel produced from the white nanocapsules was also able to absorb UV light, likely a secondary result of the amount of light that is scattered by the nanocapsules.

In a similar study, Paese and collaborators (2009) evaluated the *in vitro* efficacy of benzophenone-3 in the following forms: free incorporated into the matrix of hydrophilic gels with polysorbate 80, soluble in capric/caprylic triglycerides, associated with hydrogels containing nanocapsules, and hydrogels containing nanocapsules without actives (placebo). The results demonstrated that the light scattering produced by the unloaded nanocapsules (evaluated through light absorption) is not as effective as the UV light absorption/scattering observed in the nanocapsules containing benzophenone-3 (29). The results demonstrated in the present study corroborate the findings of Paese and collaborators.

Conclusion

In the present study, we developed spray-dried powders as an intermediate product. Although the powders presented characteristics of agglomerated microparticles, our findings demonstrated that the use of spray dryer technology improved the performance of the formulation when redispersed (HG-$NC_{A+R+TiM}$ in comparison to the HG-FREE). The results demonstrate that HG-$NC_{A+R+TiM}$ is a promising system for topical application due to its high adherence to the stratum corneum, with the absence of irritant reactions under the chorioallantoic membrane, high adhesion to the skin surface and increased photoprotection against UV radiation. In the assay of evaluation in vitro effectiveness, we highlighted the effects of the progressive combination of systems, its influence on the absorption of UV light and consequently an increase in photoprotection according to the complexity of the formulation (HG-$NC_{A+R+TiM}$ > CCTA). Finally, we emphasize the unprecedented use of the association of titanium dioxide with microalgae as drying aids in improving the finished product; it may represent a novel strategy in photoprotective formulations.

Acknowledgments

To CAPES (Coordenação de Aperfeiçoamento de Pessoal de Nível Superior) for the scholarship. To CNPQ (Conselho Nacional de Desenvolvimento Científico e Tecnológico) for the financial support. The authors would like to thank the Research Support Foundation of Rio de Grande do Sul State (FAPERGS - Brazil; PRONEX FAPERGS/CNPq 12/2014 - Grant 16/2551-0000467-6), National Council for Scientific and Technological Development (CNPq - Brazil; Grant #465687/2014-8) and National Institute of Pharmaceutical Nanotechnology (INCT-NANOFARMA - Brazil; Grant #2014/50928-2) by financial support.

Conflict of interest

The authors declare no conflicts of interest.

References

1. Kim JC, Park TJ, Kang HY. Skin-aging pigmentation: who is the real enemy? Cells. 2022; 11:1-13.
2. Salminen A, Kaarniranta K, & Kauppinen A. Photoaging: UV radiation-induced inflammation and immunosuppression accelerate the aging process in the skin. Inflammation Research, 2022; 71: 817-831.
3. Wei M, He X, Liu N, et al. Role of reactive oxygen species in ultraviolet-induced photodamage of the skin. Cell division, 2024; 19: 1-9.
4. Guterres SS, Paese K, Pohlmann AR. Polymeric Nanoparticles. In Nanoparticles for Biomedical Applications, editors. 1st ed. Amsterdam: Elsevier; 2020. p. 73–94.
5. Tampucci S, Burgalassi S, Chetoni P, Monti D. Cutaneous permeation and penetration of sunscreens: formulation strategies and in vitro methods. Cosmetics., 2018; 5:1-14.
6. Berenbeim JA, Wong NG, Cockett MC, Berden C, Oomens J, Rijs AM, Dessent CE. Unravelling the Keto-Enol Tautomer Dependent Photochemistry and Degradation Pathways of the Protonated UVA Filter Avobenzone. J Phys Chem A. 2020; 124:2919-2930.
7. Sharma A, Kuhad, A, Bhandari R. Novel nanotechnological approaches for treatment of skin-aging. Journal of tissue viability. 2022; 31: 374-386.
8. Tian B, Liu J. Resveratrol: a review of plant sources, synthesis, stability, modification, and food application. J Sci Food Agric. 2020; 100: 1392-1404.
9. Detoni C, Souto GD, da Silva ALM, Pohlmann AR, Guterres S. S. Photostability and Skin Penetration of Different E-Resveratrol-Loaded Supramolecular Structures. Photochem Photobiol. 2012; 88: 913-921.
10. Coradini K, Lima FO, Oliveira CM, Chaves PS, Athayde ML, Carvalho LM, Beck RCR. Co-

encapsulation of resveratrol and curcumin in lipid-core nanocapsules improves their in vitro antioxidant effects. Eur J Pharm Biopharm. 2014; 88:178-185.
11. Davies S, Contri RV, Guterres SS, Pohlmann AR, Külkamp IC. Simultaneous nanoencapsulation of lipoic acid and resveratrol with improved antioxidant properties for the skin. Colloids Surf B: Biointerfaces. 2020; 192: 1-10.
12. Guterres SS, Beck RCR, Pohlmann AR. Spray-drying technique to prepare innovative nanoparticulate formulations for drug administration: a brief overview. Braz J Phys. 2009; 39:205-209.
13. Vehring R, Snyder H, Lechuga-Ballesteros D. Spray Drying. In: Ohtake S, Izutsu K, Lechuga-Ballesteros D, editors. Drying Technologies for Biotechnology and Pharmaceutical Applications. 1st ed. 2020. p.179-216.
14. Sarrate R, Ticó JR, Miñarro M, Carrillo C, Fàbregas A, García-Montoya E, Pérez-Lozano P, Suñé-Negre JM. Modification of the morphology and particle size of pharmaceutical excipients by spray drying technique. Powder Technol. 2015; 270:244-255.
15. Müller CR, Bassani VL, Pohlmann AR, Michalowski CB, Petrovich PR, Guterres SS. Preparation and Characterization of Spray-Dried Polymeric Nanocapsules. Drug Dev Ind Pharm. 2000; 26:343–347.
16. Tang D, Han W, Li P, Miao X, Zhong J. CO2 biofixation and fatty acid composition of Scenedesmus obliquus and Chlorella pyrenoidosa in response to different CO2 levels. Bioresource Technol. 2011; 102:3071-3076.
17. Ren H, Liu B, Ma C, Zhao L, Ren N. A new lipid-rich microalga Scenedesmus sp. strain R-16 isolated using Nile red staining: effects of carbon and nitrogen sources and initial pH on the biomass and lipid production. Biotechnol Biofuels. 2013; 6: 1-10.
18. Almeida GF, de Araújo PH, Florentino AC,. Bezerra RM, Carvalho JC, Faustino SM, Ferreira IM. Fatty acid ethyl esters from microalgae of *Scenedesmus ecornis* by enzymatic and acid catalysis. Quim Nova. 2018; 41:1-4.
19. Ariede MB, Candido TM, Jacome ALM, Velasco MVR, Carvalho JCM, Baby AR. Cosmetic attributes of algae-A review. Algal Res. 2017; 25: 483-487.
20. Bicudo CEM, Menezes M. Gêneros de algas de águas continentais do Brasil: chave para identificação e descrições. 2 ed. São Carlos: RiMa, 2006. p. 502
21. Venturini CG, Jäger E, Oliveira CP, Bernardi A, Battastini AM, Guterres SS, Pohlmann AR. Formulation of lipid core nanocapsules. Colloids Surf A. 2011; 375: 200-208.
22. Puglia C, Damiani E, Offerta A, Rizza L, Tirendi GG, Tarico MS, Curreri S, Bonina F, Perrotta RE. Evaluation of nanostructured lipid carriers (NLC) and nanoemulsions as carriers for UV-filters: characterization, in vitro penetration and photostability studies. Eur J Pharm Sci. 2014; 51:211-217.
23. Frozza RL, Bernardi A, Hoppe JB, Meneghetti AB, Battastini AMO, Pohlmann AR, Guterres SS, Salbego C. Lipid-core nanocapsules improve the effects of resveratrol against Aβ-induced neuroinflammation. J Biomed Nanotechnol. 2013; 9:2086-2104.
24. Külkamp IC, Rabelo BD, Bertilz SJ, Isoppo M, Bianchin MD, Schaffazick SR, Pohlmann AR, Guterres SS Nanoencapsulation improves the in vitro antioxidant activity of lipoic acid. J Biomed Nanotechnol., 2011; 7: 598-607.
25. Silva ALM, Contri RV, Jornada DS, Pohlmann AR, Guterres SS. Vitamin K1–loaded lipid-core nanocapsules: physicochemical characterization and in vitro skin permeation. Skin Res Technol. 2013; 19:223-230.
26. Katzer T, Chaves P, Bernardi A, Pohlmann AR, Guterres SS, Beck RCR. Prednisolone-loaded nanocapsules as ocular drug delivery system: development, in vitro drug release and eye toxicity. J Microencapsul. 2014; 31 :1-10.
27. Luepke NP. Hen's eggs chorioallantoic membrane test for irritation potential. Food Chem Toxicol. 1985; 23:287–91.
28. Contri RV, Katzer T, Ourique AF, da Silva ALM, Beck RCR, Pohlmann AR, Guterres SS. Combined effect of polymeric nanocapsules and chitosan hydrogel on the increase of capsaicinoids adhesion to the skin surface. J Biomed Nanotechnol. 2013; 9:1-11.
29. Paese K, Jäger A, Poletto FS, Pinto EF, Rossi-Bergmann B, Pohlmann AR, Guterres SS. Semisolid formulation containing a nanoencapsulated sunscreen: effectiveness, in vitro photostability and immune response. J Biomed Nanotechnol. 2009; 5:240-246.
30. Sant'Anna CL, Tucci A, Azevedo MTP, Melcher SS, Werner VR, Malone CFS, Rossini EF, Jacinavicius FR, Hentschke GS, Osti JAS, Santos KRS, Gama-Júnior WA, Rosal C, et al. Atlas de cianobactérias e microalgas de águas continentais brasileiras. São Paulo: Instituto de Botânica; 2012. p. 175.
31. Zanella L, Alam MA. Extracts and Bioactives from Microalgae (Sensu Stricto): Opportunities and Challenges for a New Generation of Cosmetics. In: Alam A, Xu JL, Wang Z, editors. Microalgae Biotechnology for Food, Health and High Value Products. Springer, Singapore; 2020.p. 295-349.
32. Hoshina R, Hayakawa MM, Kobayashi M, Higuchi R, Suzaki T. Pediludiella daitoensis gen. et sp. nov. (Scenedesmaceae, Chlorophyceae), a large coccoid green alga isolated from a Loxodes ciliate. Sci Rep. 2020; 10:1-13.
33. Akgül F, Kizilkaya IT, Akgül R, Erduğan H. Morphological and molecular characterization of Scenedesmus-like species from Ergene River Basin

(Thrace, Turkey). Turk J Fish Aquat Sc. 2017; 17:609-619.
34. Fiel LA, Paese K, Rizzi M, Guterres SS, Pohlmann AR. A strategy to estimate the intrinsic flux of a poorly water-soluble substance for comparison with its release from lipid-core nanocapsules. Colloids Surf A Physicochem Eng Asp. 2014; 441: 16-724.
35. Schmid-Wendtner MH, Korting HC. The pH of the skin surface and its impact on the barrier function. Skin Pharmacol Physiol. 2006; 19:296-302.
36. Bianchin MD, Külkamp-Guerreiro IC, de Oliveira CP, Contri RV, Guterres SS, Pohlmann AR. Radar charts based on particle sizing as an approach to establish the fingerprints of polymeric nanoparticles in aqueous formulations. J Drug Deliv Sci Tec. 2015; 30:180-189.
37. Kockler J, Robertson S, Oelgemöller M, Davies M, Bowden B, Brittain HG, Glass BD. Butyl methoxy dibenzoylmethane. In: Profiles of Drug Substances, Excipients and Related Methodology. Academic Press. 2013; 33:87-111.
38. Oliveira CP, Venturini CG, Donida B, Poletto FS, Guterres SS, Pohlmann AR. An algorithm to determine the mechanism of drug distribution in lipid-core nanocapsule formulations. Soft Matter. 2013; 9:1141-1150.
39. R. C. R. Beck, A. F. Ourique, S. S. Guterres, A. R. Pohlmann. Spray-dried polymeric nanoparticles for pharmaceutics: a review of patents. Recent Pat Drug Deliv Formul. 2012195-208.
40. de Andrade DF, Vukosavljevic B, Hoppe JB, Pohlmann AR, Guterres SS, Windbergs M, Külkamp IC, Salbego Cg, R. Beck RCR. Redispersible Spray-Dried Powder Containing Nanoencapsulated Curcumin: The Drying Process Does Not Affect Neuroprotection In vitro. AAPS PharmSciTech. 2019: 20:283.
41. Marchiori MCL, Ourique AF, C. da Silva CB, Raffin RP, Pohlmann AR, Guterres SS, Beck RCR. Spray-Dried Powders Containing Tretinoin-Loaded Engineered Lipid-Core Nanocapsules: Development and Photostability Study. J Nanosci Nanotechnol. 2012; 11:1–9.
42. Lewicka ZA, Benedetto AF, Benoit DN, William Y, Fortner JD, Colvin VL. The structure, composition, and dimensions of TiO_2 and ZnO nanomaterials in commercial sunscreens. J Nanoparticle Res. 2011; 20: 1-10.
43. Verdurmen REM, Houwelingen GV, Gunsing M , Verschueren M, Straatsma J. Agglomeration in spray drying installations (the EDECAD project): Stickiness measurements and simulation results. Drying Technology. 2006; 24:721-726.
44. Cardoso AM, de Oliveira EG, Coradini K, Bruinsmann KA, Aguirre T, Lorenzoni R, Barcelos RCR, Roversi K, Rossato DR, Pohlmann AR, Guterres SS, Burger ME, Beck RCR. Chitosan hydrogels containing nanoencapsulated phenytoin for cutaneous use: Skin permeation/penetration and efficacy in wound healing. Mat Sci Eng C. 2019; 96:205-217.
45. Contri RV, Soares RM, Pohlmann AR, Guterres SS. Structural analysis of chitosan hydrogels containing polymeric nanocapsules. Mat Sci Eng C. 2014; 42:234-242.
46. Johnson JW, Bergfeld, Belsito WWF, Hill DV, Klaassen RA, Liebler CD, Gill DC. L. J. Safety Assessment of Lecithin and Other Phosphoglycerides as Used in Cosmetics. Int J Toxicol. 2020; 39:5S-25S.
47. National Center for Biotechnology Information. PubChem Compound Summary for CID 26042, Titanium dioxide. https://pubchem.ncbi.nlm.nih.gov/compound/Titanium-dioxide. Accessed Mar 8, 2020.
48. Stout HS, Murphy KA. Skin rejuvenation and defense system. United States patent US 9925137. 2018 Mar 27.
49. Lapasin R. Rheological Caracterization of Hydrogels. In: P. Matricardi, F. Alhaique, T. Coviello, editors. Polysaccharide hydrogels: Characterization and biomedical applications. 1st ed. New york: CRC Press,; 2016. p. 83-138
50. Alves MP, Raffin RP, Fagan SB. Rheological Behavior of Semisolid Formulations Containing Nanostructured Systems. In: Beck R, Guterres S, Pohlmann A. editors. Nanocosmetics and Nanomedicines. Springer Science & Business Media; 1st ed. Porto Alegre: Springer;2011 p. 37-45.
51. Bettoni CC, Felippi CC, de Andrade C, Raffin RP, Jager A, Guterres SS, Costa TD. Isotretinoin-loaded nanocapsules: stability and cutaneous penetration by tape stripping in human and pig skin. J Biomed Nanotechnol. 2012; 8:258-271.
52. F. C. Flores, J. A. De Lima, C. R. Da Silva, D. Benvegnú, J. Ferreira, M. E. Burger, R. C. R. Beck, C. M. B. Rolim, M. I. U. M. Rocha, M. L. Veiga, C. D. B. Da Silva. Hydrogels containing nanocapsules and nanoemulsions of tea tree oil provide antiedematogenic effect and improved skin wound healing. J Nanosci Nanotechnol. 2015; 15:800-809.
53. Pereira RL, Leites FI, Paese K, Sponchiado RM, Michalowski CB, Guterres SS, Schapoval EE. Hydrogel containing adapalene-and dapsone-loaded lipid-core nanocapsules for cutaneous application: development, characterization, in vitro irritation and permeation studies. Drug Dev Ind Pharm. 2016; 42:001-2008.
54. Baby DK. Rheology of hydrogels. In: Thomas S, Sarathchandran C, Chandran N, editors. Rheology of Polymer Blends and Nanocomposites. 1st ed. Amsterdam: Elsevier; 2020 p. 193-204.
55. Carvalho FC, Calixto G, Hatakeyama IN, Luz GM, Gremião MPD, M. Chorilli. Rheological, mechanical, and bioadhesive behavior of hydrogels to optimize skin delivery systems. Drug Dev Ind Pharm. 2013; 39:1750-1757.

56. Chen Y. Properties and development of hydrogels. In: Chen Y, editor. Hydrogels Based on Natural Polymers. 1st ed. Amsterdam: Elsevier; 2020 p.3-16.
57. Zuglianello C, Andrade PD, Chaves PS, Rigo LA, Pohlmann AR, Guterres SS, Beck RCR. Redispersible spray-dried nanocapsules for the development of skin delivery systems: proposing a novel blend of drying adjuvants. Soft Materials.2018; 16:20-30.
58. Terroso T, Külkamp IC, Jornada DS, Pohlmann AR, Guterres SS. Development of semi-solid cosmetic formulations containing coenzyme Q10-loaded nanocapsules. Lat Am J Pharm. 2009; 28:819-26.
59. Machado ACHR, Lopes PS, Raffier CP, Haridass IN, Roberts M, Grice J, Leite-Silva VR. Skin Penetration. In: Sakamoto K, Lochhead RY, Maibach HI, Yamashita Y. editors. Cosmetic Science and Technology: Theoretical Principles and Applications. 1st ed. Amsterdam: Elsevier; 2017. p. 741-755.
60. Osterwalder U, Sohn M, Herzog B. Global state of sunscreens. Photodermatol Photoimmunol Photomed. 2014; 30:62-80.
61. Thiers S, Tasseau O. Les cosméceutiques: cosmétiques ou médicaments? Le MiDiFABs. 2005 3:47-56.
62. Guterres SS, Alves MP, Pohlmann AR. Polymeric nanoparticles, nanospheres and nanocapsules, for cutaneous applications. Drug Target Insights. 2007; 2:147-157.
63. H. Gonzalez. Percutaneous absorption with emphasis on sunscreens. Photochem Photobiol Sci. 2010; 9:482-488.
64. Santos JS. Desenvolvimento de formulações contendo filtros solares nanoencapsulados. 2014 204 f. (Doutorado em Nanotecnologia Farmacêutica) – Universidade Federal do Rio Grande do Sul – RS, 2014.
65. Cozzi AC, Perugini P, Gourion-Arsiquaud S. Comparative behavior between sunscreens based on free or encapsulated UV filters in term of skin penetration, retention and photo-stability. Eur J Pharm Sci. 2018; 121:309-318.
66. Batista-Dhuarte A, Murillo GJ, Betancourt JE, Oliver P, Damiana T. The Hen's Egg Test on Chorioallantoic Membrane: An alternative assay for the assessment of the irritating effect of vaccine adjuvants. Int J Toxicol. 2016; 35:627-633.
67. Barbosa TC, Nascimento LED, Bani C, Almeida T, Nery M, Santos RS, Menezes LRO, Zielinska A, Fernandes AR, Cardoso JC, Jäger A, Jäger E, Sanchez-Lopez E, Nalone L, Souto EB, Severino P. Development, Cytotoxicity and Eye Irritation Profile of a New Sunscreen Formulation Based on Benzophenone-3-poly (ε-caprolactone) Nanocapsules. Toxics 2019; 7:1-12.
68. Contri RV, Fiel LA, Alnasif N, Pohlmann AR, Guterres SS, Schäfer-Korting M. Skin penetration and dermal tolerability of acrylic nanocapsules: influence of the surface charge and a chitosan gel used as vehicle. Int J Pharm. 2016; 507:12-20.
69. Jain SK, Jain NK. Multiparticulate carriers for sun-screening agents. Int J Cosmet Sci. 2010; 32:89-98.
70. Detoni CB, Paese K, Beck RCR, Pohlmann AR, Guterres SS. Nanosized and Nanoencapsulated Sunscreens. In: Beck RCR, Guterres SS, Pohlmann AR, editors. Nanocosmetics and Nanomedicines. 1st ed. Springer Science & Business Media; 2011. p. 333-362.
71. Schaffazick SR, Pohlmann AR, Dalla-Costa T, Guterres SS. Freeze-drying polymeric colloidal suspensions: nanocapsules, nanospheres and nanodispersion. A comparative study. Eur. J. Pharm. Biopharm. 2003; 53: 501-505.

CC BY NC SA